Article

Supplementary Information: First steps towards understanding the non-linear impact of Mg on calcite solubility; A molecular dynamics study

Janou A. Koskamp[1], Sergio E. Ruiz Hernandez[1], Nora H. De Leeuw[1,2] and Mariette Wolthers[1]*

[1] Department of Earth Sciences, Utrecht University, 3584 CB Utrecht, The Netherlands; j.a.koskamp@uu.nl (J.A.K.); s.e.ruizhernandez@uu.nl (S.E.R.H.); n.h.deleeuw@leeds.ac.uk (N.H.D.L.)

[2] School of Chemistry, University of Leeds, Leeds LS2 9JT, UK

* Correspondence: m.wolthers@uu.nl; Tel.: +31302535042

Force field

All potential parameters used in this study are listed in Table S1 [1–3].

Table S1. Potential parameters.

Water (SPC/fw)			
Species		**Molecule/Atom**	**Charge (e)**
Mg		Magnesium	+2.000
Ca		Calcium	+2.000
Cc		Carbon from carbonate	+1.135
Oc		Oxygen from carbonate	-1.045
Ow		Oxygen from water	-0.820
Hw		Hydrogen from water	+0.410
Bond styles		k **(ev Å^{-2})**	r_0 **(Å)**
Cc—Oc	Harmonic	40.8493	1.012
Ow—Hw	Harmonic	45.9296231	1.012
Angle styles		k **(ev rad^{-2})**	Θ_0
Hw— Ow — Hw	Harmonic	3.29134	113.24

		Θ_0	K_2 **(ev rad^{-2})**	K_3 **(ev rad^{-2})**	K_4 **(ev rad^{-2})**
Oc— Cc — Oc	class2	120.0	6.617	0.0	0.0
		M (ev Å^{-2})	r_1 **(Å)**	r_2 **(Å)**	
Oc— Cc — Oc	class2 bb	12.818	1.3042	1.3042	
		N_1 **(ev Å^{-2})**	N_2 **(ev Å^{-2})**	r_1 **(Å)**	r_2 **(Å)**
Oc— Cc — Oc	class2 ba	1.53319	1.53319	1.3042	1.3042

Improper styles		K_2 **(ev rad^{-2})**	K_4 **(ev rad^{-2})**
Oc— Cc — Oc-Oc	distance	13.647	360.0
Interatomic interactions			
Lennard-Jones Potential		ε **(eV)**	σ **(Å)**
Ow — Ow		0.006739769454	3.165492
Ca—Ow *		0.000950	3.35
Mg—Ow *		0.001137	2.82

Buckingham Potential	**A (eV)**	ϱ **(Å)**	**C (eV Å^6)**
Oc—Ow *	12534.455133	0.202	12.09
Oc—Hw *	396.0	0.217	0.0

Ca—Oc *	3161.6335	0.271511	0.0
Ca—Cc *	120000000	0.12	0.0
Oc— Oc *	63840.199	0.198913	27.89901
Mg—Oc *	3944.8613	0.23816	0.0

*The interaction was set to zero over the range 6 – 9 Å

Umbrella sampling

An example of and input file used to perform the steered MD calculations prior to the umbrella sampling:

```
UNITS LENGTH=A
p: POSITION ATOM=1191
dx: COMBINE ARG=p.x PERIODIC=-47.70,47.70
MOVINGRESTRAINT ...
 ARG=dx
 STEP0=0      AT0=40.7 KAPPA0=0.0
 STEP1=1000    AT1=41.2  KAPPA1=20000.0
 STEP2=2000    AT2=41.7  KAPPA2=20000.0
 STEP3=3000    AT3=42.2  KAPPA3=20000.0
 STEP4=4000    AT4=42.7  KAPPA4=20000.0
 STEP5=5000    AT5=43.2  KAPPA5=20000.0
 STEP6=6000    AT6=43.7  KAPPA6=20000.0
 STEP7=7000    AT7=44.2  KAPPA7=20000.0
 STEP8=8000    AT8=44.7  KAPPA8=20000.0
 STEP9=9000    AT9=45.2  KAPPA9=20000.0
 STEP10=10000 AT10=45.7  KAPPA10=20000.0
 STEP11=11000 AT11=46.2  KAPPA11=20000.0
 STEP12=12000 AT12=46.7  KAPPA12=20000.0
 STEP13=13000 AT13=47.2  KAPPA13=20000.0
 STEP14=14000 AT14=47.7  KAPPA14=20000.0
 STEP15=15000 AT15=48.2  KAPPA15=20000.0
 STEP16=16000 AT16=48.7  KAPPA16=20000.0
 STEP17=17000 AT17=49.2  KAPPA17=20000.0
 STEP18=18000 AT18=49.7  KAPPA18=20000.0
 STEP19=19000 AT19=50.2  KAPPA19=20000.0
 STEP20=20000 AT20=50.7  KAPPA20=20000.0
 STEP21=21000 AT21=51.2  KAPPA21=20000.0
 STEP22=22000 AT22=51.7  KAPPA22=20000.0
 STEP23=23000 AT23=52.2  KAPPA23=20000.0
 STEP24=24000 AT24=52.7  KAPPA24=20000.0
 STEP25=25000 AT25=53.2  KAPPA25=20000.0
 STEP26=26000 AT26=53.7  KAPPA26=20000.0
 STEP27=27000 AT27=54.2  KAPPA27=20000.0
 STEP28=28000 AT28=54.7  KAPPA28=20000.0
 STEP29=29000 AT29=55.2  KAPPA29=20000.0
 STEP30=30000 AT30=55.7  KAPPA30=20000.0
 STEP31=31000 AT31=56.2  KAPPA31=20000.0
 STEP32=32000 AT32=56.7  KAPPA32=20000.0
 STEP33=33000 AT33=57.2  KAPPA33=20000.0
 ... MOVINGRESTRAINT

 PRINT ARG=* STRIDE=100 FILE=COLVAR
```

After the steered MD, the different frames with the calcium at different positions above the surface were taken as the input configuration for the different umbrella calculations. Below an example of an umbrella calculation

```
UNITS LENGTH=A
p: POSITION ATOM=1191
dx: COMBINE ARG=p.x PERIODIC=-47.70,47.70
dy: COMBINE ARG=p.y PERIODIC=-23.984,23.984
dz: COMBINE ARG=p.z PERIODIC=-20.150,20.150
RESTRAINT ARG=dx AT=40.7 KAPPA=48.2
RESTRAINT ARG=dy AT=23.89 KAPPA=482.0
RESTRAINT ARG=dz AT=8.91 KAPPA=482.0
PRINT ARG=* STRIDE=10 FILE=COLVAR
```

To evaluate if there was a satisfactory overlap between the sampling of the umbrellas a histogram was constructed. **Error! Reference source not found.** shows an example of the histograms obtained over all the umbrellas used to construct the energy profile. The higher intensities indicate the stronger spring constant of that umbrella. All systems showed similar overlap.
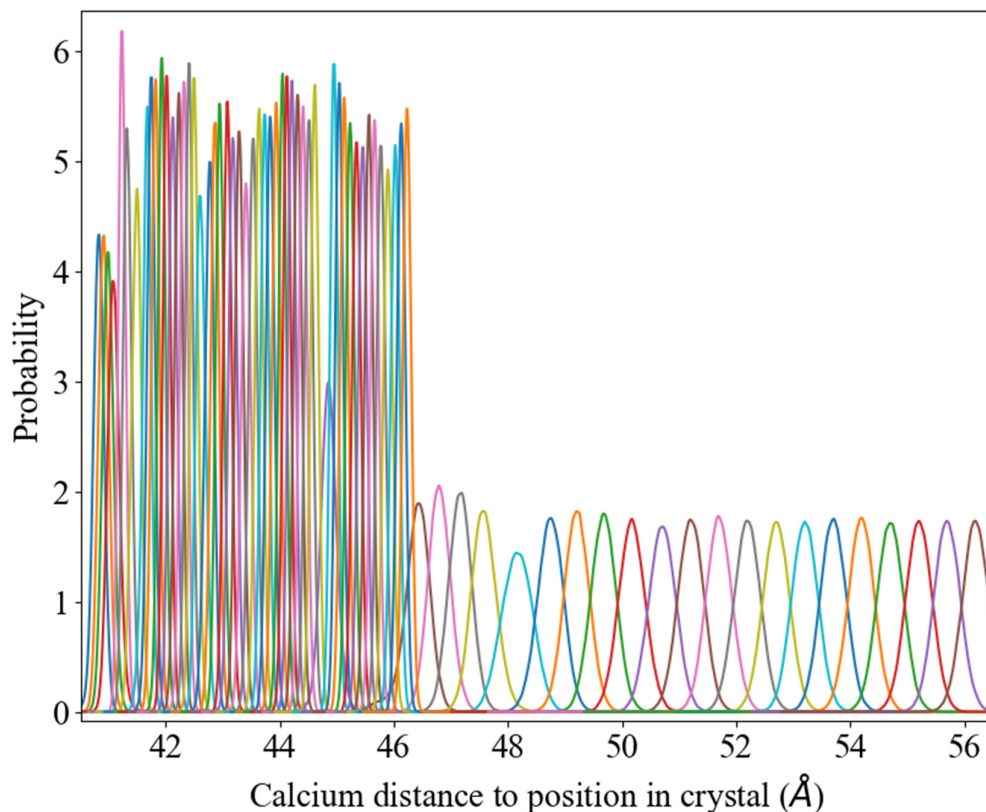
Figure 1. An example of the histograms obtained from all umbrellas placed along the CV,.

Water dipole angle relative to the surface

The angle between the dipole of the water coordinated to the cations in the surface with the surface plane revealed the orientation of the water molecules relative to the surface. An angle of 90 degrees means that the water molecule is standing normal to the surface, with protons pointing towards the solution. An angle of zero means that a water molecule is lying parallel to the surface. As Kerisit and Parker [4] showed, this angle

changes while molecules move to or from the surface, indicating that a water molecule is rotating [4]. The dipole angles of water on top of the different surfaces are shown in Table 1 in the main text. The average angle on the HMgF calcite was 0.24° smaller compared to the average angle on the pure calcite, indicating that the water molecules were positioned (almost) perpendicular to the surface in the HMgF interface.

Vibrational spectrum

Insights in the dynamics of interfacial water were obtained from the analysis of the Vibrational Density of States (VDOS). The VDOS was taken as the sum of the Fourier transformed Velocity AutoCorrelation Function (VACF) of both oxygen and hydrogen atoms of the water. At high frequencies (**Error! Reference source not found.** on the left) the bending and stretching vibrations of water ($\sim$1500 cm^{-1} and $\sim$3700 cm^{-1}, respectively) were represented. For both, pure calcite and HMgF calcite, interfacial water (<3.5 angstrom from the surface) showed similar intramolecular vibrations. Also, the intensity and position were comparable to the VDOS of bulk water for the bending, but interfacial water expressed a little shift to a higher energy for the stretching vibration ($\sim$3700 cm^{-1}). The wavenumber range related with vibrations and librations of the hydrogen bond network were expressed in the region below 1000 cm^{-1}, with, from left to right, first the intermolecular motion of the O-O-O bonding ($\sim$ 50 cm^{-1} in bulk water), second the O–O intermolecular stretching ($\sim$ 250 cm^{-1} in bulk water) and third the intermolecular rotational modes ($\sim$300 – 1000 cm^{-1} in bulk water), **Error! Reference source not found.** is a zoom in this region. The vibrational modes representing the H-bond network of interfacial water on top of pure and HMgF calcite system were shifted towards higher energies compared to bulk water. Also, the intermolecular stretching of the hydrogen bond is more pronounced ($\sim$400 cm^{-1}) compared to a pure water system. The hydrogen bond network above HMgF calcite showed less intermolecular stretching and intermolecular O-O-O bonding motion. The librational (rotational) mode on the other hand was slightly more expressed in the interfacial water on top of a HMgF calcite system.
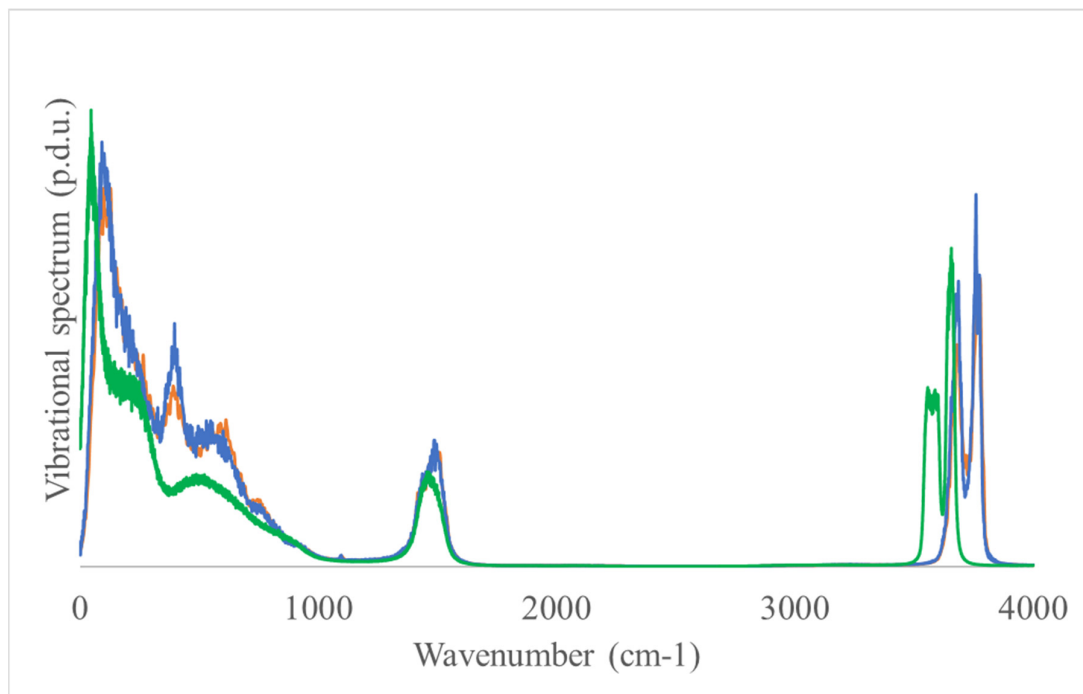
Figure 2. VDOS of interfacial water on top of a pure calcite (blue) and HMgF calcite (orange). For comparison and forcefield specific peak positions, in green the VDOS spectrum of pure bulk water.
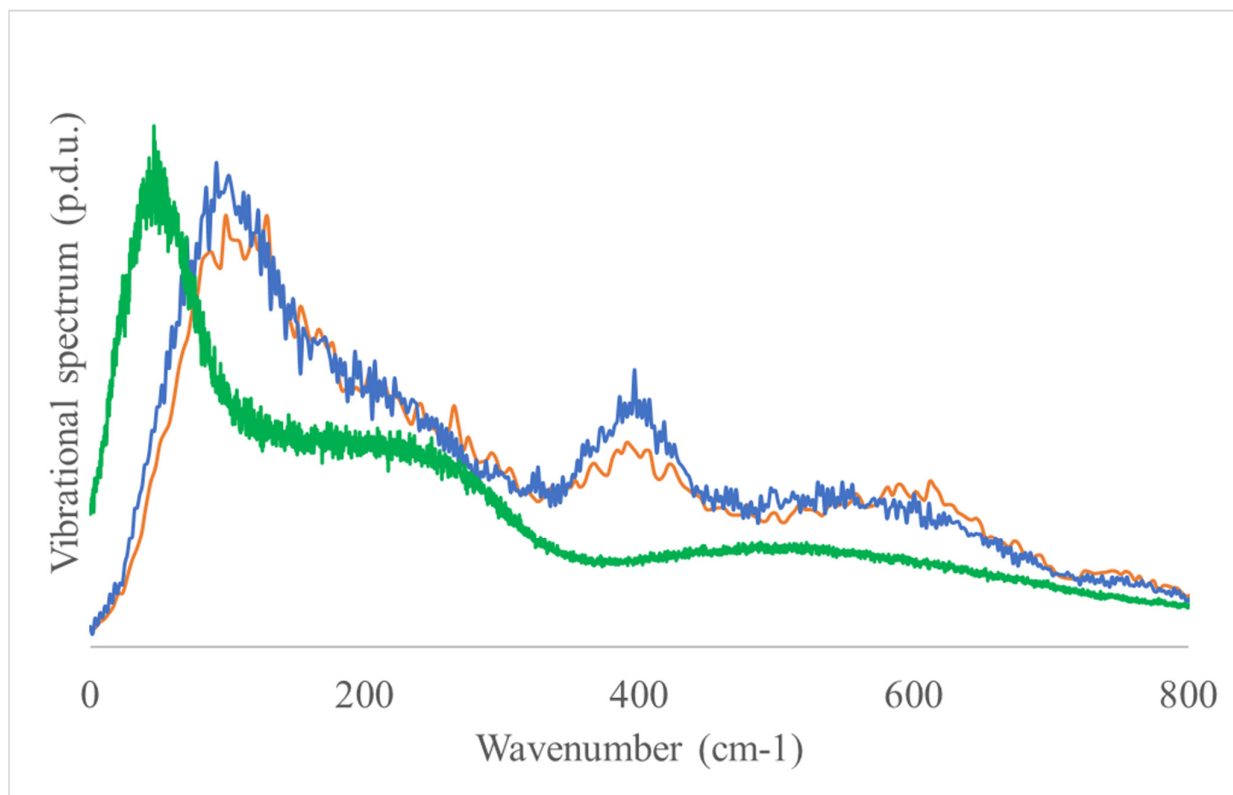
Figure 3. Zoom of VDOS spectrum range related to characteristics of the hydrogen bond network. Interfacial water on top of a pure calcite (blue) and HMgF calcite (orange). Pure bulk water (green).

Exchange frequency and diffusion coefficient

The average exchange frequency of water in the coordination shell of Ca^{2+} in the flat surface is shown in **Error! Reference source not found.**. The number of exchanges per ns near surface calcium ions was higher when Mg^{2+} was present in the surface. Because Mg^{2+} was randomly distributed over the surface, local environment could vary strongly, from calcium ions without any Mg^{2+} in the direct vicinity to being fully surrounded by Mg^{2+}. To visualize, the variation in exchange frequency on top of pure and HMgF is shown in **Error! Reference source not found.** and **Error! Reference source not found.**. The range of exchange frequencies of water on top of pure calcite and low Mg^{2+} calcite varied from 6 to 54 ns^{-1} while the range for HMgF calcite is wider and goes from 6 to 98 ns^{-1}. In addition, the diffusion coefficient of the interfacial water (set at a thickness of 0.350 nm, based on the first minimum in the $Ca^{2+} — Ow$ RDF for calcium in solution) was calculated and shown in Table 1 in the main text. The three components (x, y and z) were split. This way we can exclude the diffusion perpendicular (z-axis) to the surface, because, due to the small finite size in the z direction, the accuracy of the diffusion coefficient in this direction is very low. As can be seen in the table, the diffusion coefficient parallel to the surface was higher when water was in contact with HMgF calcite. Apart from that, the diffusion along the x-axis was, in both pure and HMgF calcite, approximately two times the diffusion coefficient along the y-axis. Along the x-axis, the distance between two cations was around 0.490 nm while the distance between two cations along the y-axis was 0.398 nm.

Table 2. Average exchange frequencies and diffusion coefficients of water coordinated to Ca^{2+} in a flat calcite surface.

System	$N_{ex} \cdot ns^{-1}$	D_x (10^{-9} m²s⁻¹)	D_y (10^{-9} m²s⁻¹)	D_z (10^{-9} m²s⁻¹)
Pure calcite	25.7	0.031	0.017	0.003
Low Mg^{2+} flat surface	24.9	0.031	0.018	0.003
High Mg^{2+} flat surface	31.4	0.046	0.022	0.004
Values from literature				
Pure_DM[a]	78			
Pure_SF[b]	0.52			
Pure_ST[c]	3.3	0.6	0.6	>0.2
Pure_ME[d]	-	0.1	0.1	-

[a] Obtained using Direct method [5]; [b] Obtained using Survival Function [6]; [c] Diffusion obtained using short (5 ps) trajectories [4]; [d] Obtained using the modified Einstein equation [7].
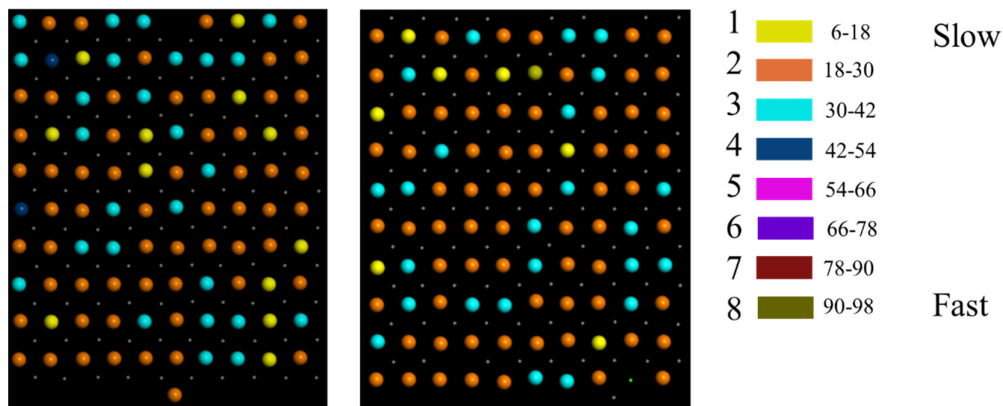
Figure 4. Variation in exchange frequency of water on top of pure calcite. The colours follow the exchange frequencies indicated in the legend. The highest Nex found in pure calcite was 54 s⁻¹·
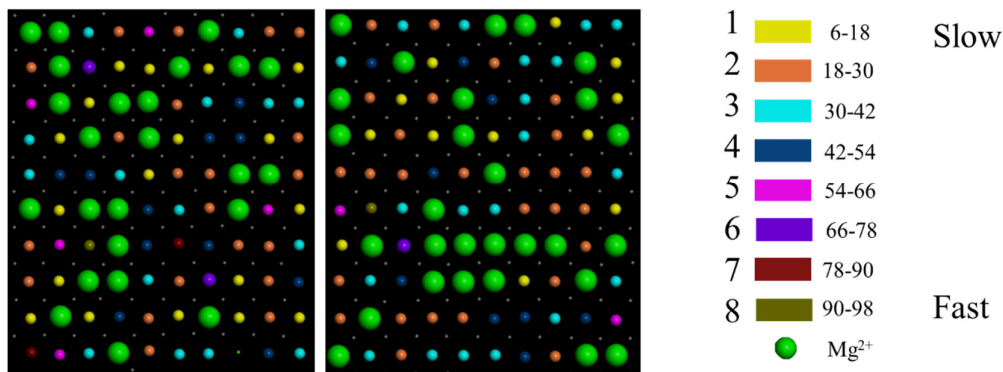
Figure 5. Variation in exchange frequency of water on top of HMgF calcite. The colours follow the exchange frequencies indicated in the legend. The green spheres represent Mg^{2+} as indicated with the red arrow, where no exchanges occurred over the course of the simulations.

Dynamic surface energies and bulk distances

The dynamic surface energies (Table S2) showed the same trend as the surface energy of the dry systems (Table 2 in the main text). However, the difference between the systems is less subtle with the dynamic surface energy of HMgI being almost twice as high as the

flat surfaces. In addition, the standard deviation was higher for the slabs with an island on top, where PureI had a standard deviation closer to the flat surfaces than to HMgI.

Table S2 Surface energies of after relaxation at 300K with water on top. The U_s in equation 1 was calculated as the energy of the configuration without water

{$10\bar{1}4$} System	Surface Energies (J/m²)	Standard deviation
Pure calcite	1.75	0.013
Low Mg²⁺ flat surface	1.78	0.013
High Mg²⁺ flat surface	1.73	0.014
Island pure calcite	1.83	0.021
Island high Mg²⁺	3.25	0.036

Table S4. A summary of computed relaxed surface energies of calcite.

Surface Energies (J/m²)	Reference
0.510	[8]
0.503	[9]
0.860	[10]
0.380	[11]
0.590	[12]
0.430	[11]
0.590	[11]
0.590	[13]
0.520	[13]
0.420	[13]
0.534	[14]
0.706	[15]
0.590	[16]
0.590	[17]
0.863	[18]
0.322	[19]
0.590	[20]
0.590	[21]
0.570	[22]
0.600	[23]
0.530	[24]
0.230	[25]

To evaluate how stressed the local structure was around the extracted Ca²⁺, we compared its cation distances with the ones in the structure of pure calcite and dolomite. Average Ca²⁺ — $I^{+/-}$ distances (where $I^{+/-}$ is Oc, Ca²⁺) in LMg were equal to the pure calcite. This is illustrated by the RDF's in Figure 2a of the main text and in Table S2, where the shortest average distances in the crystal between the ions are listed.
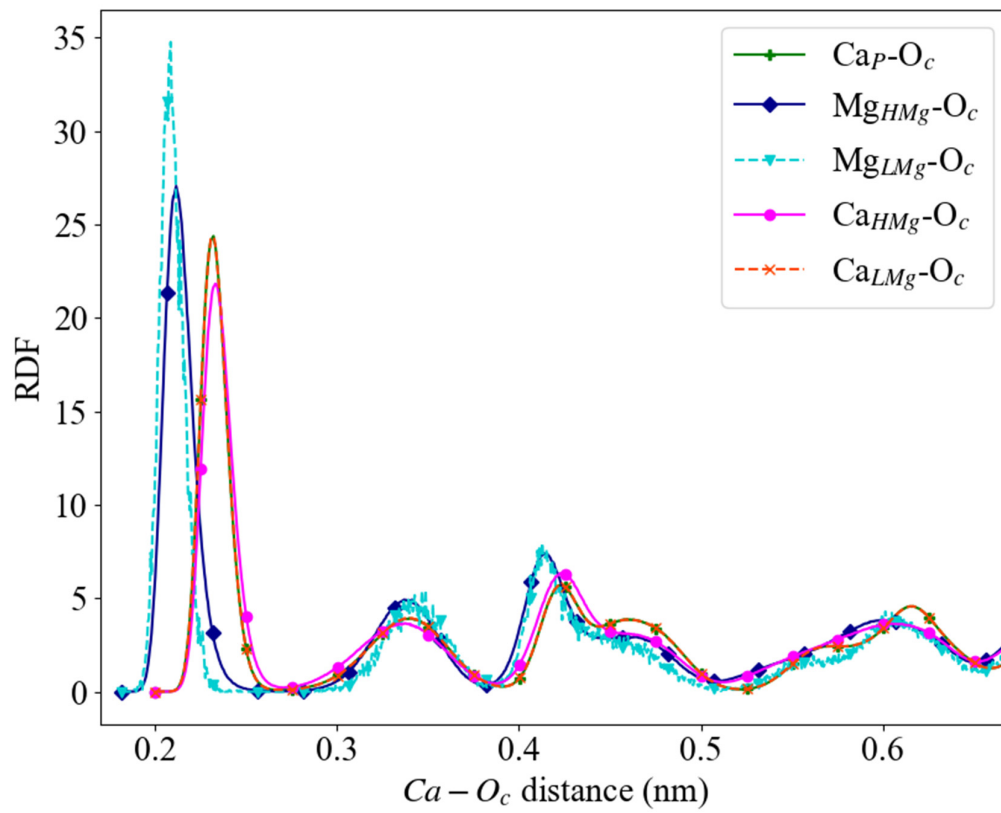
Figure S1. Radial distribution function for the cation with the oxygen of carbonate (O_c) in pure, LMg and HMg calcite crystals.

Table S3. Coordination distances in the bulk crystal structure

Element pair	Distance (nm)
Calcite	
$Ca^{2+} — Ca^{2+}$ (c-axis)*	0.405; 0.411±0.020
$Ca^{2+} — Ca^{2+}$ (b-axis)*	0.499; 0.505±0.023
$Ca^{2+} — Oc$*	0.233; 0.233±0.006
Dolomite	
$Mg^{2+} — Ca^{2+}$	0.387
$Ca^{2+} — Ca^{2+}$	0.482
$Mg^{2+} — Oc$	0.212
$Ca^{2+} — Oc$	0.241
Low Mg^{2+} flat surface	
$Mg^{2+} — Ca^{2+}$ (c-axis)	0.388±0.014
$Mg^{2+} — Ca^{2+}$ (b-axis)	0.491±0.025
$Ca^{2+} — Ca^{2+}$ (c-axis)	0.411±0.020
$Ca^{2+} — Ca^{2+}$ (b-axis)	0.505±0.023
$Mg^{2+} — Oc$	0.209±0.006
$Ca^{2+} — Oc$	0.233±0.007
High Mg^{2+} flat surface	
$Mg^{2+} — Ca^{2+}$ (c-axis)	0.392±0.012
$Mg^{2+} — Ca^{2+}$ (b-axis)	0.485 ±0.012
$Ca^{2+} — Ca^{2+}$ (c-axis)	0.400±0.013
$Ca^{2+} — Ca^{2+}$ (b-axis)	0.479±0.013
$Mg^{2+} — Oc$	0.213±0.007
$Ca^{2+} — Oc$	0.235±0.008

*the second reported distance is the value retrieved form our own simulations

LMg local distances

Table S6. Relevant distances between surface calcium and the neighbouring atoms and calcium coordination numbers at the different Ca^{2+} positions near Mg^{2+} in the low Mg^{2+} {10$\bar{1}$4} calcite surface.

Element pair	Distance to Mg^{2+} (nm)	Distance to Ca^{2+} (nm)	Distance to O_c (nm)
Ca_{LMgF1}	0.3925	0.3975; 0.4525;0.4925 0.6275	0.2325
Ca_{LMgF2}	0.4525	0.3975; 0.4875; 0.6325	0.2325
Ca_{LMgF3}	0.6225	0.3975; 0.4975; 0.6325	0.2325
Ca_{LMgF4}	0.7975	0.3975; 0.5175; 0.6325	0.2325

Surface with an island
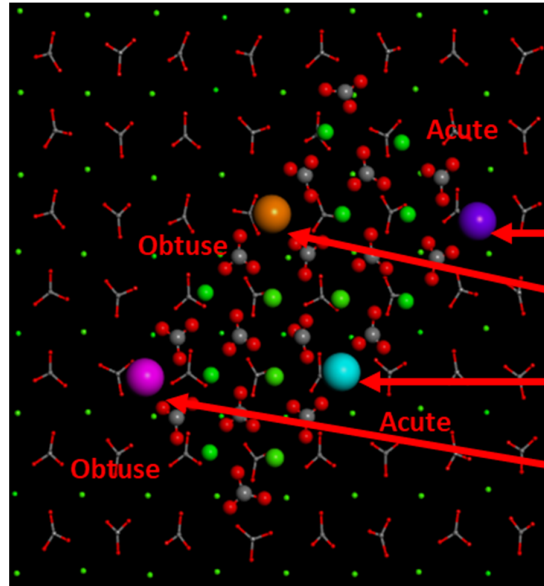
Figure 7. Top view of the 4x8 atoms island on top of Pure {10$\bar{1}$4} surface carbonate groups in grey (C) and red (O) and Ca^{2+} in small green or colour and symbol coded larger spheres to link them to the free energy profiles (Figure 5b) in orange (obtuse edge, ▬), turquoise (acute edge, ▼), pink (obtuse corner, ●) and purple (acute corner, ■).

Table 7. Comparison of relevant distances and coordination in the surface of PureI versus HMgI. Between the selected calcium (**Error! Reference source not found.**) and the neighbouring atoms.

Element pair	Distance (nm)	Coordination Number (<0.350 nm*)
Calcium acute corner		
Ca$_{PAC}$ — *Oc*	0.2375	4.02
Ca$_{HMgIAC}$ — *Oc*	0.2325	4.03
Ca$_{PAC}$ — *Ow*	0.2375	4.38
Ca$_{HMgIAC}$ — *Ow*	0.2375	4.96
Ca$_{HMgIAC}$ — *Nearest Mg^{2+} on island*	0.4125	
Ca$_{PAC}$ — *Nearest Ca^{2+} on island*	0.4325	
Ca$_{HMgIAC}$ — *Second Mg^{2+} on island*	0.6375	
Ca$_{PAC}$ — *Second Ca^{2+} on island*	0.6225	
Calcium obtuse corner		
Ca$_{POC}$ — *Oc*	0.2375	5.04
Ca$_{HMgIOC}$ — *Oc*	0.2325	5.66
Ca$_{POC}$ — *Ow*	0.2375	3.94
Ca$_{HMgIOC}$ — *Ow*	0.2325	4.02
Ca$_{HMgIOC}$ — *Nearest Mg^{2+} on island*	0.3875	
Ca$_{POC}$ — *Nearest Ca^{2+} on island*	0.4075	
Ca$_{HMgIOC}$ — *Second Mg^{2+} on island*	0.6075	
Ca$_{POC}$ — *Second Ca^{2+} on island*	0.6325	
Calcium acute edge		
Ca$_{PAE}$ — *Oc*	0.2375	5.09
Ca$_{HMgIAE}$ — *Oc*	0.2325	5.12
Ca$_{PAE}$ — *Ow*	0.2375	3.50

$Ca_{HMgIAE} — Ow$	0.2325	4.03
$Ca_{HMgIAE} — Nearest\ Ca^{2+}\ on\ island$	0.4075	
$Ca_{HMgIAE} — Nearest\ Ca^{2+}\ on\ island$	0.4425	
$Ca_{PAE} — Nearest\ Ca^{2+}\ on\ island$	0.4325	
$Ca_{HMgIAE} — Second\ Mg^{2+}\ on\ island$	0.5775	
$Ca_{HMgIAE} — Second\ Ca^{2+}\ on\ island$	0.6075	
$Ca_{HMgIAE} — Second\ Ca^{2+}\ on\ island$	0.6575	
$Ca_{PAE} — Second\ Ca^{2+}\ on\ island$	0.6225	
Calcium obtuse edge		
$Ca_{POE} — Oc$	0.2325	5.45*
$Ca_{HMgIOE} — Oc$	0.2325	4.70*
$Ca_{POE} — Ow$	0.2325	2.20*
$Ca_{HMgIOE} — Ow$	0.2325	2.37*
$Ca_{HMgIOE} — Nearest\ Mg^{2+}\ on\ island$	0.4025	
$Ca_{HMgIOE} — Nearest\ Ca^{2+}\ on\ island$	0.5025	
$Ca_{POE} — Nearest\ Ca^{2+}\ on\ island$	0.4383	
$Ca_{HMgIOE} — Second\ Mg^{2+}\ on\ island$	0.5925	
$Ca_{HMgIOE} — Second\ Mg^{2+}\ on\ island$	0.6325	
$Ca_{HMgIOE} — Second\ Ca^{2+}\ on\ island$	0.6275	
$Ca_{POE} — Second\ Ca^{2+}\ on\ island$	0.6375	

*For calcium in the obtuse edge (Ca_{POE} and Ca_{HMgIOE}) a cut off of 0.30 nm was used for the coordination number. Based on the first minimum in the corresponding RDF's.

References

1. Raiteri, P.; Gale, J.D.; Quigley, D.; Rodger, P.M. Derivation of an Accurate Force-Field for Simulating the Growth of Calcium Carbonate from Aqueous Solution: A New Model for the Calcite−Water Interface. *J. Phys. Chem. C* **2010**, *114*, 5997–6010, doi:10.1021/jp910977a.
2. Raiteri, P.; Demichelis, R.; Gale, J.D. Thermodynamically Consistent Force Field for Molecular Dynamics Simulations of Alkaline-Earth Carbonates and Their Aqueous Speciation. *J. Phys. Chem. C* **2015**, *119*, 24447–24458, doi:10.1021/acs.jpcc.5b07532.
3. Wu, Y.; Tepper, H.L.; Voth, G.A. Flexible simple point-charge water model with improved liquid-state properties. *J. Chem. Phys.* **2006**, *124*, 024503, doi:10.1063/1.2136877.
4. Kerisit, S.; Parker, S.C. Free energy of adsorption of water and metal ions on the {10Ī4} calcite surface. *J. Am. Chem. Soc.* **2004**, *126*, 10152–10161, doi:10.1021/ja0487776.
5. Wolthers, M.; Di Tommaso, D.; Du, Z.; De Leeuw, N.H. Variations in calcite growth kinetics with surface topography: molecular dynamics simulations and process-based growth kinetics modelling. *CrystEngComm* **2013**, *15*, 5506, doi:10.1039/c3ce40249e.
6. De La Pierre, M.; Raiteri, P.; Gale, J.D. Structure and Dynamics of Water at Step Edges on the Calcite {1014} Surface. *Cryst. Growth Des.* **2016**, *16*, 5907–5914, doi:10.1021/acs.cgd.6b00957.
7. Mutisya, S.M.; Kirch, A.; De Almeida, J.M.; Sánchez, V.M.; Miranda, C.R. Molecular Dynamics Simulations of Water Confined in Calcite Slit Pores: An NMR Spin Relaxation and Hydrogen Bond Analysis. *J. Phys. Chem. C* **2017**, *121*, 6674–6684, doi:10.1021/acs.jpcc.6b12412.
8. Akiyama, T.; Nakamura, K.; Ito, T. Atomic and electronic structures of surfaces. *Phys. Rev. B - Condens. Matter Mater. Phys.* **2011**, *84*, 085428, doi:10.1103/PhysRevB.84.085428.
9. Bruno, M.; Massaro, F.R.; Prencipe, M.; Aquilano, D. Surface reconstructions and relaxation effects in a centre-symmetrical crystal: The {00.1} form of calcite (CaCO3). *CrystEngComm* **2010**, *12*, 3626–3633, doi:10.1039/c002969f.
10. Kvamme, B.; Kuznetsova, T.; Uppstad, D. Modelling excess surface energy in dry and wetted calcite systems. *J. Math. Chem.* **2009**, *46*, 756–762, doi:10.1007/s10910-009-9548-y.
11. Kerisit, S.; Parker, S.C.; Harding, J.H. Atomistic simulation of the dissociative adsorption of water on calcite surfaces. *J. Phys. Chem. B* **2003**, *107*, 7676–7682, doi:10.1021/jp034201b.
12. De Leeuw, N.H.; Cooper, T.G. A Computer Modeling Study of the Inhibiting Effect of Organic Adsorbates on Calcite Crystal Growth. *Cryst. Growth Des.* **2004**, *4*, 123–133, doi:10.1021/cg0341003.
13. Parker, S.C.; Kerisit, S.; Marmier, A.; Grigoleit, S.; Watson, G.W. Modelling Inorganic Solids and Their Interfaces: A Combined Approach of Atomistic and Electronic Structure Simulation Techniques. *ChemInform* **2003**, *35*, no-no, doi:10.1002/chin.200406248.

14. Rohl, A.L.; Wright, K.; Gale, J.D. Evidence from surface phonons for the (2 × 1) reconstruction of the 101̄4) surface of calcite from computer simulation. *Am. Mineral.* **2003**, *88*, 921–925, doi:10.2138/am-2003-5-622.

15. Braybrook, A.L.; Heywood, B.R.; Jackson, R.A.; Pitt, K. Parallel computational and experimental studies of the morphological modification of calcium carbonate by cobalt. *J. Cryst. Growth* **2002**, *243*, 336–344, doi:10.1016/S0022-0248(02)01439-2.

16. Cooper, T.G.; De Leeuw, N.H. Adsorption of methanoic acid onto the low-index surfaces of calcite and aragonite. In Proceedings of the Molecular Simulation; Taylor & Francis Group , 2002; Vol. 28, pp. 539–556.

17. De Leeuw, N.H. Surface structures, stabilities, and growth of magnesian calcites: A computational investigation from the perspective of dolomite formation. *Am. Mineral.* **2002**, *87*, 679–689, doi:10.2138/am-2002-5-610.

18. Hwang, S.; Blanco, M.; Goddard, W.A. Atomistic simulations of corrosion inhibitors adsorbed on calcite surfaces I. Force field parameters for calcite. *J. Phys. Chem. B* **2001**, *105*, 10746–10752, doi:10.1021/jp010567h.

19. Wright, K.; Cygan, R.T.; Slater, B. Structure of the (1014) surfaces of calcite, dolomite and magnesite under wet and dry conditions. *Phys. Chem. Chem. Phys.* **2001**, *3*, 839–844, doi:10.1039/b006130l.

20. De Leeuw, N.H.; Parker, S.C. Surface Structure and Morphology of Calcium Carbonate Polymorphs Calcite, Aragonite, and Vaterite: An Atomistic Approach. *J. Phys. Chem. B* **1998**, *102*, 2914–2922, doi:10.1021/jp973210f.

21. Titiloye, J.O.; De Leeuw, N.H.; Parker, S.C. Atomistic simulation of the differences between calcite and dolomite surfaces. *Geochim. Cosmochim. Acta* **1998**, *62*, 2637–2641, doi:10.1016/S0016-7037(98)00177-X.

22. Nygren, M.A.; Gay, D.H.; Catlow, C.R.A.; Wilson, M.P.; Rohl, A.L. Incorporation of growth-inhibiting diphosphonates into steps on the calcite cleavage plane surface. *J. Chem. Soc. - Faraday Trans.* **1998**, *94*, 3685–3693, doi:10.1039/a806585c.

23. De Leeuw, N.H.; Parker, S.C. Atomistic simulation of the effect of molecular adsorption of water on the surface structure and energies of calcite surfaces. *J. Chem. Soc. - Faraday Trans.* **1997**, *93*, 467–475, doi:10.1039/a606573b.

24. Parker, S.C.; Oliver, P.M.; De Leeuw, N.H.; Titiloye, J.O.; Watson, G.W. Atomistic simulation of mineral surfaces: Studies of surface stability and growth. *Phase Transitions* **1997**, *61*, 83–107, doi:10.1080/01411599708223731.

25. Parker, S.C.; Kelsey, E.T.; Oliver, P.M.; Titiloye, J.O. Computer modelling of inorganic solids and surfaces. *Faraday Discuss.* **1993**, *95*, 75–84, doi:10.1039/FD9939500075.